Simulation of a method for forming a laser-cooled positron plasma

A. S. Newbury,* B. M. Jelenković,† J. J. Bollinger, and D. J. Wineland
Time and Frequency Division, National Institute of Standards and Technology, Boulder, Colorado 80303
(Received 13 January 2000; published 18 July 2000)

We have simulated the trapping and cooling of moderated positrons in a Penning trap in which the positrons lose energy through collisions with a simultaneously stored laser-cooled $^9Be^+$ plasma. Once the positrons are trapped, they cool through sympathetic cooling with the $^9Be^+$ plasma. After the positrons cool, their motion parallel to the magnetic field reaches a state of thermal equilibrium with the $^9Be^+$ ions and they rotate about the trap axis at the same frequency as the $^9Be^+$ ions . Therefore, a centrifugal separation will occur, forcing the positrons to coalesce into a cold column along the trap axis. A simulation which, in part, utilizes Monte Carlo techniques, indicates a capture efficiency of as high as 0.3% for 300 K moderated positrons passing through a $^9Be^+$ plasma with a density of 10^{10} atoms cm^{-3} and a column length of 1 cm. This capture efficiency leads to the positron capture rate of $\sim$1000 positrons per second, assuming a 100 mCi positron source and 10^{-3} for the efficiency for moderating positrons from the source. The resulting dense reservoirs of cold positrons may be useful for antihydrogen production and for reaching a plasma state in which the mode dynamics must be treated quantum mechanically.

PACS number(s): 32.80.Pj, 52.25.Wz

I. INTRODUCTION

With advances in the use of positron moderators to produce low-energy positron beams [1–12], and in the trapping of non-neutral plasmas [13,14], attention has been focused on trapping and cooling positrons in electromagnetic traps [2–4,9–12,15–17]. Cold positron reservoirs are useful for positron-normal matter interaction studies, such as the study of resonances in low-energy positron annihilation on molecules [4]. With sufficiently high trapping rates, cold positrons can be released from electromagnetic traps to produce cold beams of high brightness for a number of different experiments [4,6,18]. A dense gas of positrons at sufficiently low temperature also provides an example of a plasma with quantized normal modes [15,16,19]. Finally, by passing cold antiprotons through a reservoir of cold positrons, one could form antihydrogen through three-body recombination [20–22].

Several groups have successfully trapped positrons in electromagnetic traps. Schwinberg, Van Dyck, and Dehmelt used resistive cooling of the positrons in a Penning trap to achieve trapping of small numbers [23]. Gabrielse, Haarsma, and Abdullah have combined this method with a 3 mCi source and a positron moderator to trap $\sim 3\times10^4$ positrons at a rate exceeding 10^3 per hour [3]. More recently this group has been able to trap more than 10^6 positrons in 17 hours through a different method where apparently positronium in a high Rydberg state created on the surface of the moderator is field-ionized in the trap [24,25]. Conti, Ghaffari, and Steiger have also trapped positrons in a Penning trap by injecting slow positrons into the trap while ramping the trap electrostatic potential [12,26]. Mills has discussed accumulating positrons in a magnetic bottle to produce a slow positron beam [27]. Demonstration of positron trapping in a magnetic mirror by cyclotron-resonance heating has been recently demonstrated [28]. The largest number of trapped positrons ($\sim 3\times10^8$) has been reported by Surko and coworkers [4,18,29,30]. These experiments employed collisional cooling of positrons with a room-temperature buffer gas of N_2 to provide trapping and cooling. By removing the buffer gas, the base pressure is reduced to 3×10^{-10} Torr, resulting in a positron lifetime of about one hour. With a 90 mCi positron source, a trapping rate of 3×10^8 positrons in 8 min and a trapping efficiency of moderated positrons greater than 25% were achieved.

In this paper we explore the possibility of capturing and cooling positrons in a Penning trap through collisions with a simultaneously stored laser-cooled plasma of $^9Be^+$ ions. Slow positrons become trapped through Coulomb collisions with the $^9Be^+$ plasma. Once trapped, the positrons will then be sympathetically cooled by the $^9Be^+$ plasma, which can be laser-cooled to temperatures as low as 0.5 mK [31,32]. Sympathetic cooling refers to the cooling of one species through Coulomb interactions or collisions with a second, directly cooled species [32,33]. Since this technique employs high vacuum, positron annihilation will be suppressed, permitting long trap lifetimes.

One of the simplest methods to study the transport of positrons in a $^9Be^+$ plasma is the Monte Carlo method. Unlike collisions between neutral atoms, Coulomb collision deflections at large distances are important, with each of these ''distant collisions'' producing a small scattering and velocity change. In Monte Carlo simulations one can treat the problem of Coulomb collisions through the cumulative effect of a large number of small angle scattering; we have used Monte Carlo simulations to calculate the scattering angle of the moderated positron after each pass through the $^9Be^+$ plasma. The simulations were based on the expression for the probability distribution for scattering of a positron into an angle θ after a large number of collisions, assumed to occur as a positron passes through the $^9Be^+$ plasma [34,35]. Recently, Nanbu used a Monte Carlo method to derive a simple

*Permanent address: MIT Lincoln Laboratory, Lexington, MA 02420.

†Permanent address: Institute of Physics, University of Belgrade, Belgrade, Yugoslavia.

 ©2000 The American Physical Society

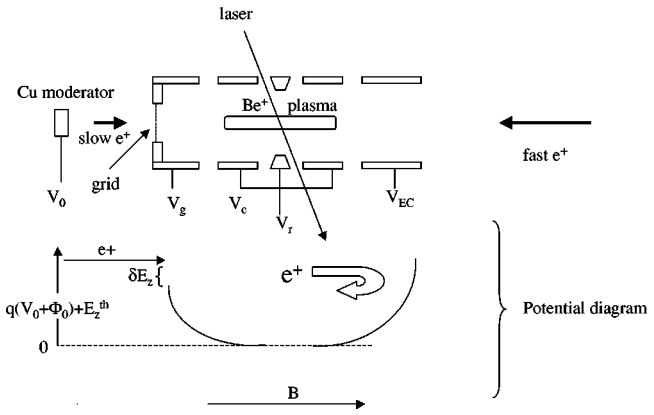

FIG. 1. Schematic diagram of a cylindrical Penning trap and of axial potentials. V_0, moderator potential; V_g, grid voltage; δE_z, positron axial kinetic energy above the grid voltage; V_r, V_c, and V_{EC}, potentials on other trap electrodes.

analytical expression for the probability density function for a deflection angle after many Coulomb collisions [36]. We also have done a number of calculations using expressions from Ref. [36] to calculate the scattering angles for positrons after passing through the plasma and obtained good agreement between the two data sets.

The basic method for capturing and cooling positrons using a $^9Be^+$ plasma, outlined previously in Ref. [16], is discussed in Sec. II. In addition, we describe here some details of a hypothetical experiment designed to trap positrons. In Sec. III we have increased the scope of the discussion by including the effects on the capture efficiency caused by the energy distribution of moderated positrons, the finite size of the positron source, the radial electric field within the plasma, and $^9Be^+$ recoil. The trap geometry, the plasma parameters, and the positron behavior described in Secs. II and III are used in the modeling of positron trapping. The Monte Carlo method used to calculate the efficiency of the proposed method [16] is described in Sec. IV. The results of the simulations and a discussion of the results are presented in Sec. V.

II. BASIC METHOD

The model assumes the $^9Be^+$ ions are first trapped in a cylindrical Penning trap contained in a room-temperature vacuum enclosure with an axial magnetic field of 6 T. Figure 1 illustrates the simple Penning trap design considered in modeling the capture of positrons. In this magnetic field, a laser-cooled $^9Be^+$ plasma in thermal equilibrium can reach a uniform density n_0 of up to 10^{10} atoms cm^{-3} [14,37]. This high density can be reached by using torques due to a laser beam [37] or due to a rotating electric-field perturbation [38,39] to control the plasma's angular momentum. A low-energy positron traversing this plasma along the magnetic-field direction will scatter off the $^9Be^+$ ions via the Coulomb interaction. The positron's parallel momentum (along the magnetic-field direction) can thus be converted to perpendicular momentum. If sufficient momentum is converted, the positron's momentum along the magnetic field can be reduced so that it will not leave the trap. In Ref. [16], it was assumed that if the positron were initially captured in this way, it would lose enough energy through cyclotron radiation to be permanently trapped. However, this is true only for a small fraction of positrons because typically, before the positron can lose enough energy through cyclotron radiation, its energy can be redistributed back by Coulomb collisions along the trap axis and it will escape [40]. In the work described here, we now include this escape process and the cooling effects of $^9Be^+$ recoil, which initially provides a more efficient cooling mechanism than cyclotron radiation.

In the Penning trap, the plasma rotates around the magnetic-field axis at a frequency ω_r. The technique of ''Doppler'' laser cooling [31,41,42] reduces the temperature of the plasma to less than 10 mK. The Debye length of the plasma can be expressed as $\lambda_D=(k_BT\epsilon_0/n_0q^2)^{1/2}$, where k_B is Boltzmann's constant, q is the ion's charge, and ϵ_0 is the permittivity of free space. At temperatures near 10 mK, the Debye length is small compared to plasma dimensions [31]. In this limit, the density of $^9Be^+$ ions can be expressed as a function of the $^9Be^+$ cyclotron frequency Ω, the plasma rotation frequency ω_r, and the $^9Be^+$ mass M_{Be}, as $n_0=2\epsilon_0M_{\mathrm{Be}}\omega_r(\Omega-\omega_r)/q^2$ [14,19,31]. The maximum achievable density is the Brillouin density, which occurs when $\omega_r=\Omega/2$ and has been achieved in laser-cooled plasmas with up to a few hundred thousand $^9Be^+$ ions in magnetic fields up to 4.5 T [37,39]. For $^9Be^+$ ions confined in a 6 T magnetic field, this limit is $n_0\simeq10^{10}$ cm^{-3}. We will assume that the magnetic field is uniform along the length of the trap.

As illustrated in Fig. 1, high-energy positrons from a ^{22}Na source are injected from the right into the trap, on the trap axis, through a cylindrical endcap. The positrons have a beta-decay endpoint energy of 545 keV, and these high-energy positrons will not significantly affect the ions in the plasma (a discussion of the interactions between hot positrons and plasma is contained in the Appendix). After passing through the plasma, the positrons strike a room-temperature crystal moderator. The positrons will thermalize by interacting with electrons and phonons in the crystal. In this ''reflection geometry,'' a small fraction (up to 10^{-3}) will avoid annihilation in the crystal and emerge as a beam of slow positrons [1,5,43] which then enter the trap [44]. At the surface of the crystal the moderated positrons have an energy determined by the crystal temperature. In addition, they are accelerated in the direction normal to the crystal surface by the work function Φ_0 of the crystal [1]. For the method of trapping positrons discussed here, the narrow distribution of thermal-energy positrons at the surface of the crystal is important. Measurements show that positrons emitted from a Cu(111) single-crystal moderator can have a narrow energy distribution whose width is reasonably consistent with thermal broadening given by the temperature of the moderator crystal [45]. In our calculations, for the purpose of the crystal work function, we assume the use of a Cu(111) crystal moderator.

After the positrons are emitted from the moderator crystal, their axial kinetic energy is assumed to be further reduced by a conducting screen with good transmission (the retarding grid of Fig. 1), which has a potential a few tenths of a volt above the moderator potential. If the moderator and

retarding grid potentials are equal, the axial energy of positrons as they pass through the grid is $\Phi_0+E_z^{\rm th}$, where $E_z^{\rm th}$ is the axial component of the positron's thermal energy at the crystal surface. The positrons will then enter the $^9Be^+$ plasma with relatively little kinetic energy. At these low energies ($\sim$few eV), positron annihilation on the $^9Be^+$ ions is made negligible by Coulomb repulsion. By adjusting the potential of the rightmost cylindrical electrode, we can ensure that the moderated positrons are reflected at the end of the plasma farthest from the moderator and pass through the plasma twice. During each pass, some of the axial energy can be converted to perpendicular energy through Coulomb collisions with the $^9Be^+$ ions , thereby preventing them from escaping back through the retarding grid. Positrons that remain trapped for many passes will lose enough energy through $^9Be^+$ recoil to remain permanently trapped. The positrons that are not trapped are assumed to strike the moderator or grid and annihilate.

Once the positrons are trapped within the laser-cooled $^9Be^+$ plasma, they will be cooled through a combination of sympathetic cooling through $^9Be^+$-e^+ Coulomb collisions and cyclotron radiation. After the positrons are cooled by the $^9Be^+$ plasma, both positrons and $^9Be^+$ ions will undergo uniform rotation at the same frequency ω_r and the positrons will be forced to the center of the rotating plasma because of their smaller mass [33,46]. In the limit of zero temperature, the edges of each plasma will be sharp, and the plasmas will separate, with the positrons forming a column of uniform density along the trap axis. If the $^9Be^+$ plasma density is significantly below the Brillouin limit, the densities for confined plasmas of e^+ and $^9Be^+$ are expected to be approximately equal and the plasma separation quite small [15,46]. This implies good thermal coupling and possible positron axial temperatures less than 10 mK. The discussion of strongly magnetized plasma equilibria by Glinsky *et al.* [47] indicates that the positron plasma axial and cyclotron degrees of freedom will be strongly decoupled in a 6 T magnetic field. Therefore, cyclotron radiation may keep the positron cyclotron temperature in near-thermal equilibrium with the trap electrodes. Here we assume the electrodes are maintained at room temperature, but the equilibrium cyclotron temperature could be reduced, for example, by cooling the electrodes to 4 K with a liquid helium bath or to lower temperature with a dilution refrigerator.

One way to experimentally detect the presence of trapped positrons could be by imaging the near-resonant 313 nm fluorescence of the $^9Be^+$ plasma and looking for the absence of $^9Be^+$ ions in the center of the plasma [16]. Other ions with charge-to-mass ratios higher than $^9Be^+$, such as $^4He^+$, H_3^+, and $^9Be^{2+}$, will also be trapped in the center of the plasma. These ions will not fluoresce at 313 nm and will therefore mimic the positron signature on the imaging tube. We anticipate that these ions could be distinguished from the positrons through their resonant response to radiation applied at the cyclotron frequency. The size of the ''hole'' in the $^9Be^+$ plasma will yield an estimate of the number of trapped positrons. With the imaging technique we estimate we can detect the presence of a single ''string'' of a few tens of positrons trapped on the axis within the $^9Be^+$ plasma [48].

III. POSITRON TRAPPING

Positrons within the Cu(111) moderator crystal rapidly thermalize to a Boltzmann velocity distribution [1]. Within the crystal, the positron velocity distribution $P(v_i)$ will conform to

$$P(v_i)\propto e^{-m_e v_i^2/2k_BT}, \tag{1}$$

where the subscript i indicates the velocity direction ($i=\hat{x},\hat{y},\hat{z}$), m_e is the positron mass, and T is the temperature of the crystal moderator. Positrons emitted from the moderator are accelerated in the direction perpendicular to the moderator surface by the crystal work function Φ_0. As indicated in Fig. 1, the positron velocity is primarily along the magnetic-field axis ($\hat{z}$) since the crystal surface is oriented perpendicular to that axis. Immediately outside the crystal the slow positrons will have an axial kinetic energy distribution,

$$P(E_z)dE_z\propto e^{-E_z-\Phi_0/k_BT}dE_z, \tag{2}$$

for $E_z\geqslant\Phi_0$. This distribution combines the probability of effusion from the moderator surface [7,49] with the acceleration at the surface due to the work function. Equivalently, we can assume the positron axial velocity at the crystal surface is selected from the distribution

$$P(v_z)\propto v_z e^{-m_e v_z^2/2k_BT}, \tag{3}$$

and then accelerated by the potential Φ_0. The grid potential can be adjusted so that the positrons have small excess axial energy (δE_z) with respect to the grid. Before reaching the plasma, the positrons will be accelerated by the plasma potential, $V_p(r)=-n_0qr^2/(4\epsilon_0)$. [For simplicity, we have assumed that we adjust the moderator and electrode potentials to make the plasma potential along the trap axis $V_p(r=0)=0$.]

We have modeled the initial collisions of the moderated positrons with the $^9Be^+$ ions in the weakly magnetized approximation where the effects of the magnetic field on the collisions are neglected. This approximation is valid as long as the positron's cyclotron rotation is less than one cycle during the time of a collision [47]. The number of cyclotron orbits during a collision can be defined as $\kappa=\Omega_c\tau$, where Ω_c is the positron cyclotron frequency and τ is the binary collision time. Therefore, we consider collisions where $\kappa<1$ [47]. For example, the minimum collision time is $\tau=\overline{b}/v$, where $\overline{b}=q^2/2\pi\epsilon_0 m_e v^2$ is the collisional distance of closest approach. For an energy of 0.1 eV, $v\simeq1.9\times10^7$ cm s^{-1}, making $\overline{b}\simeq1.4\times10^{-6}$ cm. At 6 T, $\Omega_c\simeq1.1\times10^{12}$ s^{-1}, yielding $\kappa=0.08$.

We calculate the initial capture of positrons after one pass by using the distribution for multiple small-angle Coulomb scattering [34,35]. (The cross section for multiple small-angle Coulomb scattering is typically larger than the cross section for a single large-angle scattering [50].) Below, we define a ''pass'' through the plasma as a pass back and forth (or from left to right and back in Fig. 1) ending with the

positron traveling towards the moderator crystal. As seen in Fig. 1, the positron can only leak out of the trap the way it entered.

The angular distribution for multiple small-angle Coulomb scattering can be simulated by calculating an energy-dependent rms scattering angle $\sqrt{\langle\theta^2\rangle}$ according to the Rutherford scattering formula such that [50]

$$\langle\theta^2\rangle=\frac{n_0 l q^4}{2\pi\epsilon_0^2 m_e^2 v^4}\ln\left(\frac{b_{\max}}{b_{\min}}\right). \tag{4}$$

Here l represents twice the plasma length, and $b_{\max}$ and $b_{\min}$ are the maximum and minimum impact parameters, respectively. We use $b_{\max}=v/\Omega_c$, where Ω_c is the positron cyclotron frequency and v is the magnitude of the positron velocity. The quantity $b_{\max}$ is the maximum impact parameter for which we can use the weakly magnetized approximation. It is derived by setting the parameter $\kappa=1$. For the parameters used in the above discussion of κ, $b_{\max}=0.17$ μm, which is more than an order of magnitude smaller than the mean ion spacing in the $^9Be^+$ plasma. We use $b_{\min}=\overline{b}/2$ to limit the scattering to small angles [50]. The probability of multiple scattering in one pass through an angle θ can then be approximated by a Gaussian distribution in solid angle [34,35,51],

$$P_S(\theta)d\Omega\propto\sin(\theta)\exp\left(-\frac{\theta^2}{\langle\theta^2\rangle}\right)d\theta d\phi. \tag{5}$$

This distribution is valid for multiple angle scatterings where each is less than 10° [35].

The capture of positrons within the $^9Be^+$ plasma is divided into two processes. The first process is based on Coulomb collisions and traps the positrons temporarily. After a single pass a positron can be trapped if the amount of axial energy converted into perpendicular or cyclotron energy is greater than the excess axial kinetic energy of the positron. Because of the difference in the positron and $^9Be^+$ masses, positrons will actually lose very little energy by passing once through the plasma. If initially trapped, the positron will continue to make passes through the plasma until it either escapes the trap or becomes permanently trapped. To escape the trap, a positron which is ''initially captured'' needs to convert its perpendicular energy back to axial energy.

The second process permanently traps the positrons by depleting their excess energy primarily through $^9Be^+$ recoil cooling. A positron with energy E scattering off the ions in the plasma through an angle θ will lose an energy

$$\Delta E=4E\left(\frac{m_e}{M_{\mathrm{Be}}}\right)\sin^2(\theta/2) \tag{6}$$

to $^9Be^+$ recoil. Because of the large mass difference between a $^9Be^+$ ion and a positron, a positron will have to make many transits through the plasma in order to lose its excess energy. But once sufficient positrons are trapped, other positrons can lose axial energy through e^+-e^+ collisions. The trapping efficiency under these collisions is expected to be higher than for the e^+-$^9Be^+$ collisions because of the larger energy loss due to positron recoil. This enhanced recoil cooling is not taken into account here.

IV. SIMULATION

The Monte Carlo simulation proceeds as follows. For each positron, an initial radial coordinate is chosen according to a flat distribution over the active area of the source. The initial velocities out of the moderator in the x and y directions are chosen using velocity distribution functions $P(v_i)$ of Eq. (1). The z component of the positron velocity was obtained using a modified Boltzmann distribution [Eq. (3)]. Equivalently, the velocity v_z at the surface of the crystal is determined from the equation $v_z=v_{\mathrm{th}}[-\ln(1-R_n)]^{1/2}$, where R_n is a random number between 0 and 1. Here $v_{\mathrm{th}}=\sqrt{2kT/m}$, where T is the temperature of the crystal. We use $E_z^{\mathrm{th}}=mv_z^2/2$ to denote the axial kinetic energy. At the moderator surface the positron is further accelerated in the axial direction by the surface work function. We have used the Cu(111) work function $\Phi_0=0.4$ eV in the Monte Carlo simulation.

Figure 1 illustrates the electrical potential experienced by the positrons as they travel from the moderator, held at V_0, through the grid at potential V_g, and into the $^9Be^+$ plasma. The moderated positrons with an axial energy above the retarding grid potential, $\delta E_z[=q(V_0-V_g)+\Phi_0+E_z^{\mathrm{th}}]$, follow the magnetic-field lines and accelerate into the plasma. Their radial coordinate r with respect to the trap symmetry axis does not change until they undergo a large number of collisions inside the plasma, since their cyclotron radius is less than 10^{-4} cm. At low temperature, the electric potential inside the plasma is approximately independent of the axial coordinate, and is given by $V_p(r)=-n_0 q r^2/(4\epsilon_0)$.

Coulomb scattering caused by one pass through the plasma is described by two angles, θ_s, the magnitude of the deflection angle, and ϕ_s, the orientation of the scattering around the deflection cone. The scattering angle θ_s was calculated assuming the distribution given by Eq. (5). This assumption leads to an expression for the scattering angle $\theta_s=\sqrt{\langle\theta^2\rangle[-\ln(R_\theta)]}$, where $\langle\theta^2\rangle$ is the rms scattering angle given by Eq. (4). Since the positron has no preferred azimuthal orientation, ϕ_s was obtained at the end of the pass from a uniform distribution $2\pi R_\phi$. Here R_θ and R_ϕ are random numbers between 0 and 1. At the end of each pass, the new values of the v_x, v_y, v_z were calculated from θ_s, ϕ_s, and the change of energy [Eq. (6)]. A test was then made to determine if the positron was permanently trapped. If this is not the case, the positron will either make another pass or is lost. By repeating these ''runs,'' we determine the percentage of moderated positrons trapped within the plasma. Typically, the Monte Carlo runs had 1.5×10^5 positrons.

V. RESULTS AND DISCUSSION

Results for the efficiency of trapping positrons in a $^9Be^+$ plasma for particular conditions are shown in Fig. 2. In this case the plasma radius was 0.1 mm, and the density was 10^{10} cm^{-3}. We chose the moderator potential to be V_0

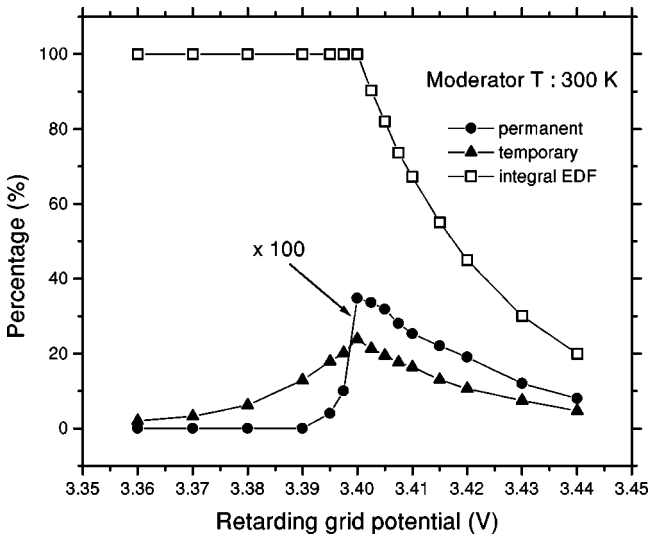

FIG. 2. Fraction of moderated positrons entering the trap (integral EDF) along with the fraction of temporarily and permanently captured positrons as a function of the retarding grid voltage for $V_0=3$ V. The crystal work function was 0.4 eV and the temperature was 300 K. The $^9Be^+$ plasma parameters were as follows: density $n_0=10^{10}$ cm^{-3}, length $l=1$ cm, and radius $r_0=0.1$ mm. Squares, integral energy distribution of positrons; circles, permanently trapped; triangles, temporarily trapped.

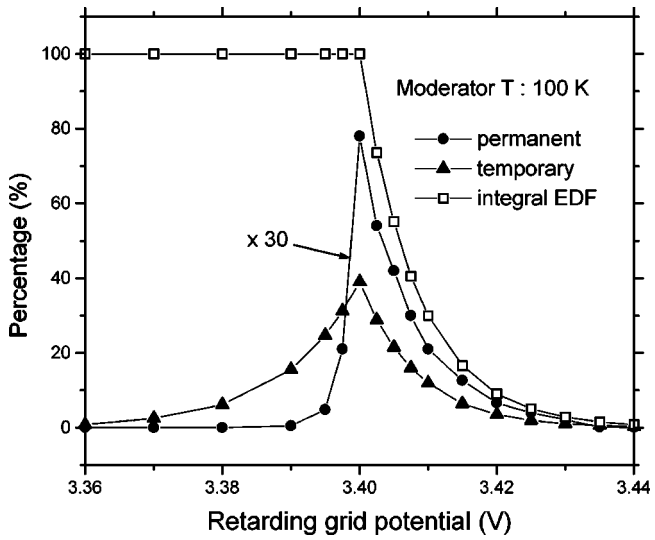

FIG. 3. Same as in Fig. 2 but for a moderator temperature of 100 K.

$=3$ V, while the grid potential V_g was varied around $V_0+\Phi_0=3.4$ V. The percentage of temporarily trapped (triangles) and permanently trapped (circles) positrons is plotted as a function of V_g. Also shown (squares) is the fraction of positrons entering the trap vs the retarding grid potential. This curve is the integral distribution of the axial component of kinetic energy, E_z. For the results of Fig. 2, the temperature of the crystal was taken to be 300 K. The maximum efficiency for positron trapping occurs at $V_g=3.4$ V and was $\sim 0.4\%$ for permanent and 24% for temporary trapping only. The results of the trapping efficiencies for the crystal cooled to 100 K are shown in Fig. 3. The width of the energy distribution is reduced by a factor of 3. Such thermal narrowing has been confirmed in experiments [7]. The efficiency for permanent trapping increases to $\sim 2.5\%$. Figures 2 and 3 indicate, as mentioned previously, that the energy spread of the moderated positrons is important for the trapping method simulated here. Experimental studies have reported near-thermal energy spreads for metal, single-crystal moderators [7,45]. In practice this condition may not be straightforward to obtain. Figure 4 shows the trapping efficiency for an energy spread of the moderated positrons corresponding to $T=2000$ K. The factor of 7 increase in the positron energy spread of Fig. 4 over Fig. 2 has resulted in a factor of 40 decrease in the efficiency for permanently trapping positrons.

In Fig. 5 we show the fraction of captured positrons for different bias potentials V_0 of the moderator while holding the crystal temperature (300 K) and plasma parameters (density, length, and radius) constant. For each value of V_0 in Fig. 5, the grid voltage was set to the value $V_g=V_0+0.4$ V which maximizes the trapping efficiency. The data show that the efficiency for permanent trapping has a maximum of $\sim 0.45\%$ when V_0 is at about 4 V. While we do not have a detailed understanding of the location of this maximum, we can describe some effects which could produce it. Once temporarily trapped, a positron will leave the plasma if it enters the loss cone θ_c about the z axis defined by $\sin(\theta_c)=\sqrt{\delta E_T/E_T}$, where E_T is the total positron kinetic energy in the plasma and δE_T is the excess kinetic energy the positron must lose to be trapped. A positron with a larger kinetic energy and the same excess energy has a smaller loss cone, which tends to increase the efficiency of trapping positrons with increasing energy. However, the energy loss per pass of a positron decreases with energy. This increases the number of passes required to permanently trap a positron (see discussions below), and will tend to decrease the trapping efficiency with increasing energy.

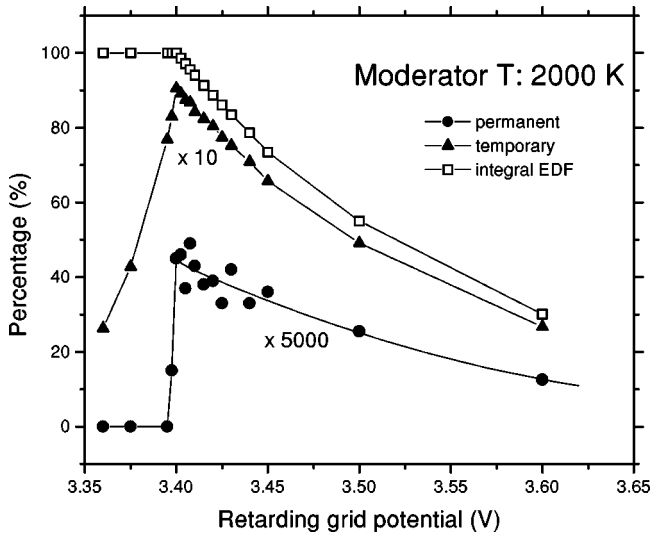

FIG. 4. Same as in Fig. 2 but for a moderator temperature of 2000 K.

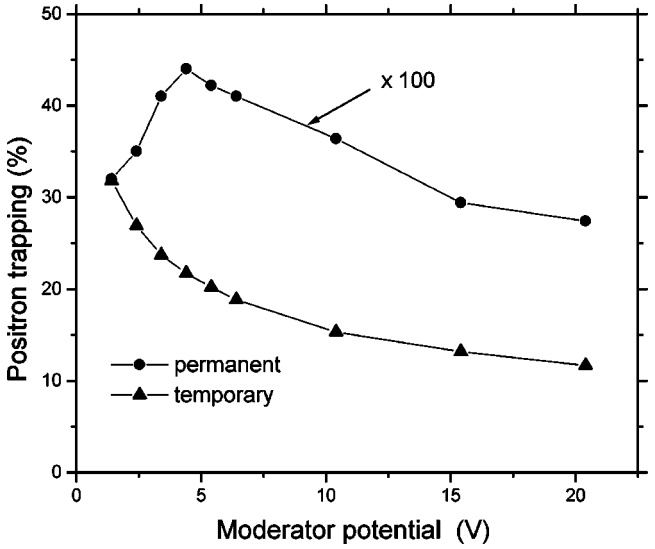

FIG. 5. Capture percentage of permanently trapped (circles) and temporarily trapped (triangles) positrons as a function of V_0. The moderator work function was 0.4 eV and grid potential was always $V_G = V_0 + 0.4$. ($n_0 = 10^{10}$ cm^{-3}, $l = 1$ cm, and $r_0 = 0.1$ mm.)

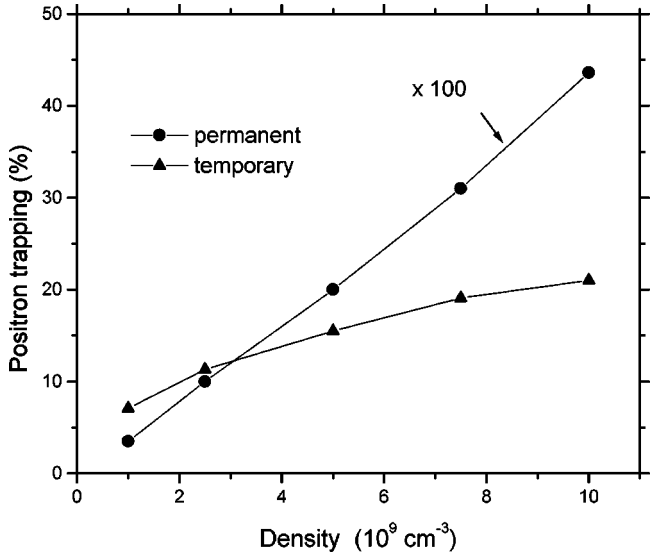

FIG. 7. Capture percentage of permanently trapped (circles) and temporarily trapped (triangles) positrons as a function of $^9Be^+$ plasma density ($r_0 = 0.1$ mm, $l = 1$ cm, $V_0 = 4$ V, and $V_g = 4.4$ V).

Shown in Figs. 6 and 7 are the variations in efficiencies for trapping positrons as the $^9Be^+$ plasma length and density were changed. The percentage of temporarily trapped positrons is increasing as a square root of both length and density. The probability for temporarily trapping positrons depends on the final scattering angle θ, which in turn is proportional to $\sqrt{\ln}$. The percentage of permanently trapped positrons is increasing linearly with n and l, possibly because the energy loss for permanent trapping [Eq. (6)] varies as the square of the rms scattering angle.

The efficiency for trapping positrons decreases with increasing plasma radius, as shown in Fig. 8, for the same reason that it decreases with increasing moderator potential V_0 for $V_0 > 4$ V (see Fig. 5). At larger radii, the positrons will have correspondingly larger energies entering the plasma. Throughout this manuscript we assume that the source radius is equal to the plasma radius.

The number of round trips in the plasma before the positron either exits back through the grid or is permanently trapped varies with the positron excess energy, values of V_0 and V_g, and the plasma radius. The histogram in Fig. 9 shows the fraction of trapped positrons vs the number of passes the positrons made through the $^9Be^+$ plasma before

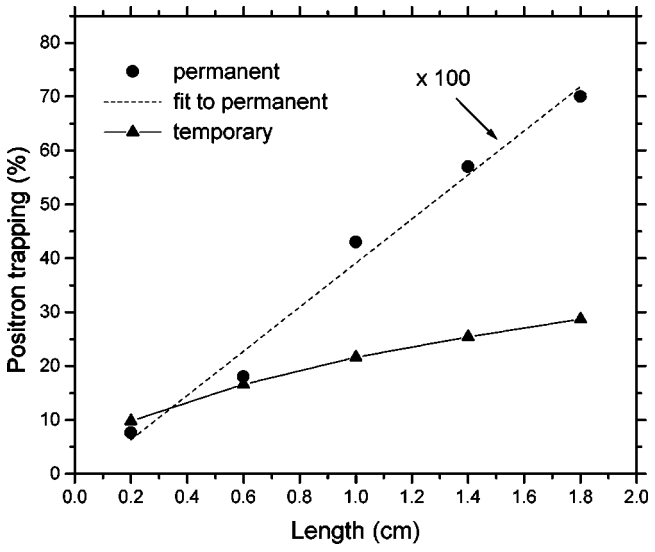

FIG. 6. Capture percentage of permanently trapped (circles) and temporarily trapped (triangles) positrons as a function of $^9Be^+$ plasma length ($n_0 = 10^{10}$ cm^{-3}, $r_0 = 0.1$ mm, $V_0 = 4$ V, and $V_g = 4.4$ V).

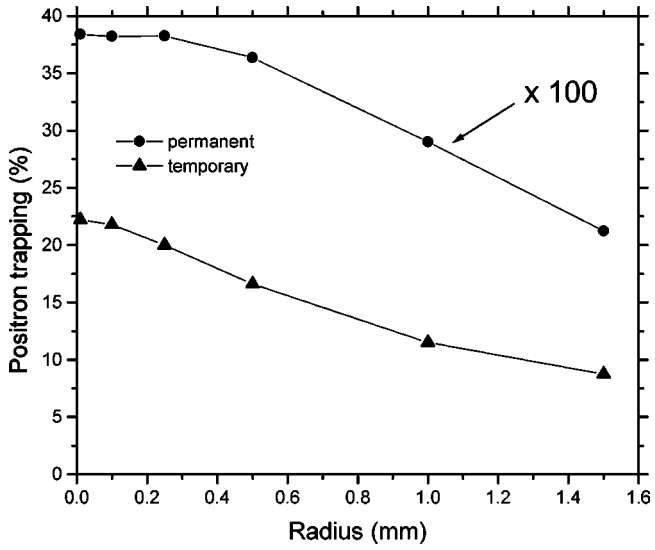

FIG. 8. Capture percentage of permanently trapped (circles) and temporarily trapped (triangles) positrons as a function of the radius of the $^9Be^+$ plasma ($n_0 = 10^{10}$ cm^{-3}, $l = 1$ cm, $V_0 = 4$ V, and $V_g = 4.4$ V). We assume the positron source radius equals the plasma radius.

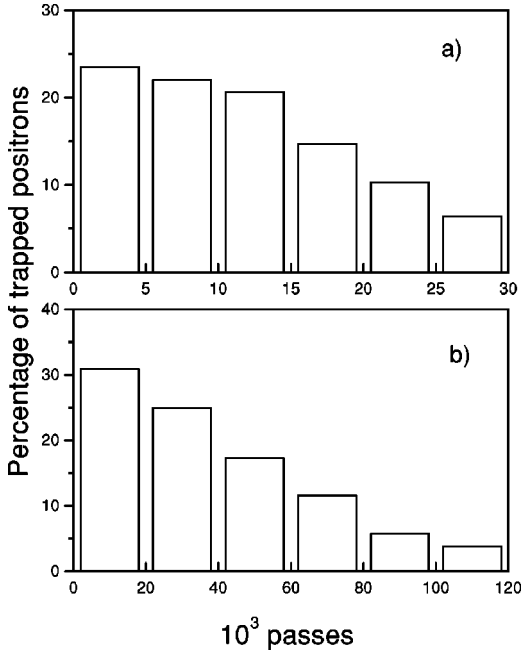

FIG. 9. Histogram showing the fraction of permanently trapped positrons vs the number of passes the positrons made through the $^9Be^+$ plasma before being trapped, for $n_0=10^{10}$ cm^{-3}, $l=1$ cm, $r_0=0.1$ mm, and $T=300$ K. (a) $V_0=4$ V, $V_G=4.4$ V; (b) $V_0=10$ V, $V_G=10.4$ V.

being permanently trapped. The results are shown for a plasma radius of 0.1 mm and for two moderator potentials, $V_0=3$ V ($V_g=3.4$ V) [Fig. 9(a)] and $V_0=10$ V ($V_g=10.4$ V) [Fig. 9(b)]. Although the positrons have the same excess energy as they pass the grid in Figs. 9(a) and 9(b), they spend different times in the trap before being captured because they enter the plasma with different kinetic energies. Similar increases in the number of passes were obtained when the plasma radius was increased to 0.5 mm. The plasma potential decreases as $-r^2$ and therefore positrons entering the plasma at larger radius have higher energies.

We can estimate the overall capture rate given the results of the simulation by including an estimate of both the source and the moderator efficiencies. A 100 mCi source will isotropically produce positrons at a rate of 3×10^9 s^{-1}. Only a fraction of the emitted positrons will reach the moderator crystal. We expect the positron flux at the Cu crystal to be $\sim4\times10^8$ s^{-1} [24]. Assuming a moderator efficiency of 10^{-3} and the trapping efficiency of 0.3%, we get a trapping rate of about 1300 positrons per second.

Using the method outlined in this paper, it should be possible to achieve a low-temperature, high-density positron plasma. In a magnetized, uncorrelated plasma, the antihydrogen recombination rate should scale as $n^2T^{-9/2}$ [20]. In a correlated plasma (plasma exhibiting liquidlike and solidlike behavior), this dependence will likely be modified. Furthermore, a pressure of 1.3×10^{-8} Pa (10^{-10} torr) may provide positron lifetimes longer than 5 days (see the Appendix). Since the Brillouin limit to the plasma density increases as the square of the magnetic field, it is possible to increase these trapping efficiencies further by going to larger magnetic fields.

We note that other electrode geometries can replace the transparent retarding grid. Any geometry which provides a potential hill between the moderator and the $^9Be^+$ plasma can mimic the effects of the retarding grid. In an experiment, a geometry other than a grid is desirable because azimuthal asymmetries in the retarding grid potential near the plasma might limit the ultimate $^9Be^+$ plasma density [14,37].

In this manuscript we assume that the $^9Be^+$ ions recoil from positron impact as if they were free particles. In fact, laser-cooled ion plasmas are often strongly coupled and exhibit liquidlike or solidlike behavior where an ion is bound in a local potential well. However, because the collision time of the weakly magnetized collisions considered here is fast compared to the period of any of the ion's plasma-mode frequencies, in considering their recoil we may treat the $^9Be^+$ ions as if they were free particles.

In addition to the importance of achieving a relatively low-temperature thermal energy spread of the moderated positrons, perhaps the largest uncertainty in an experiment designed along these lines is the ability to produce high-density, laser-cooled $^9Be^+$ plasmas of sufficient length. While large-number plasmas ($\simeq10^9$ ions [52]) and high-density plasmas ($n\simeq10^{10}$ cm^{-3} [37]) have been achieved in Penning traps, the combination of these two parameters has not yet been experimentally realized. In recent experiments we have been able to reach the Brillouin limit with $\sim10^6$ ions in a 4.5 T and 6 T magnetic field [39,53]. It may also be possible to ''stack'' a series of shorter plasmas in separate traps along the magnetic field, thereby maintaining high density and increasing the effective column length. However, even with a modestly sized single plasma, it should be possible to trap a sufficient number of positrons to evaluate the effectiveness of this technique.

ACKNOWLEDGMENTS

Support for this research was provided by the Office of Naval Research. We thank Travis Mitchell and Tom Heavner for their comments on the manuscript.

APPENDIX

It is important to discuss interactions between the energetic positrons from the ^{22}Na source and the cold $^9Be^+/e^+$ plasma. Here, we examine $^9Be^+$ loss due to positron impact ionization, plasma heating caused by the positron beam, and the loss of trapped positrons due to interactions with background gas. For simplicity we assume a 200 keV monoenergetic positron beam (the peak energy of the ^{22}Na beta-decay distribution) from an isotropic 2 mCi source and a $^9Be^+$ plasma of 1 cm length, with a 1 mm diameter and a density of 10^{10} ions cm^{-3} ($\sim8\times10^7$ ions).

The probability of an individual scattering event between a positron and a $^9Be^+$ ion can be expressed as $P=n_0\sigma l'$, where n_0 is the ion number density, σ is the event cross section, and l' is the effective path length through the plasma. Since positrons are emitted from the source isotro-

pically, many will have initial velocities perpendicular to the magnetic-field direction. These positrons will spiral along the magnetic-field lines. Spiraling through the plasma will increase the path length of these particular ions through the plasma. We can eliminate the positrons with the largest effective path lengths by electrically retarding the positron beam from the ^{22}Na source. By placing a potential hill of 1400 V between the source and the plasma, we can prohibit the positrons with the longest path lengths from making it to the plasma. Eliminating only $\sim 9\%$ of the positrons in this manner, we reduce the average path length through the plasma to $2.4l$. The calculations below for $^{9}Be^{+}$ heating and loss assume this effective path length.

1. $^{9}Be^{+}$ loss

The energetic positrons from the ^{22}Na source can doubly ionize the $^{9}Be^{+}$ plasma through electron impact ionization. $^{9}Be^{2+}$ will remain trapped but can be only sympathetically cooled; its presence can decrease the cooling capacity of the ion plasma by reducing the number of laser-cooled ions. The cross section for second ionization of Be^{+} through 200 keV electron impact is approximately [54]

$$\sigma(Be^{+}+e^{-}\rightarrow Be^{2+}+2e^{-})\simeq 3.1\times 10^{-17}\ \text{cm}^2. \quad \text{(A1)}$$

We assume the electron-impact and positron-impact ionization cross sections are approximately equal for positrons of this high energy [55]. Using this cross section and a total flux of positrons R_{e^+} of $1.3\times 10^{7}\ \text{s}^{-1}$, the number density of $^{9}Be^{+}$ ions n_0, and the average path length through the plasma $2.4l$, we can estimate the loss rate of $^{9}Be^{+}$ ions as

$$R_{Be^{2+}}=2.4\ln_0\sigma R_{e^+}\approx 11\ \text{s}^{-1}. \quad \text{(A2)}$$

At this rate, 7% of the initial 8×10^{7} $^{9}Be^{+}$ ions would be lost in about 6 days.

Another mode of $^{9}Be^{+}$ loss is through high-energy positron annihilation on the $^{9}Be^{+}$ ions. The cross section for positrons with 200 keV of kinetic energy to annihilate on $^{9}Be^{+}$ is approximately 3×10^{-25} cm^2 [56]. Thus loss of $^{9}Be^{+}$ through this mechanism caused by positrons from the ^{22}Na source is negligible.

2. $^{9}Be^{+}$ plasma heating

High-energy positrons passing through a cold dense $^{9}Be^{+}$ plasma can heat the plasma via Coulomb collisions. Since our plasma is simultaneously laser cooled, it is necessary that the rate of laser cooling be larger than that of the positron heating. To estimate the heating rate, we perform a calculation of nonrelativistic scattering. Since the heating from positron-positron collisions dominates over collisions between positron and $^{9}Be^{+}$, we estimate the heating rate due to trapped positron recoil. A high-energy positron scattering through an angle θ will impart an energy $E(\theta)=(1/2)m_e v^2\sin^2(\theta)$ to the trapped positron. We can estimate the rate of plasma heating $\dot{E}_H$ by integrating,

$$\dot{E}_H=2\pi nNv\int_{\theta_M}^{\pi/2}E(\theta)\frac{d\sigma}{d\theta}\sin\theta d\theta, \quad \text{(A3)}$$

where n is the density of positrons in the beam, v is their velocity, N is the number of positrons in the plasma, and θ_M is the minimum scattering angle for which the weakly magnetized approximation is valid [47]. This corresponds to an impact parameter approximately equal to the positron beam radius. In this limit, we estimate a heating rate of $\dot{E}_H\simeq 4.1\times 10^{-8}$ eV/s for each positron in the plasma. If we assume a positron column plasma 1 mm in diameter and 1 cm in length containing 8×10^{7} positrons, the plasma heating rate will be 3.3 eV/s.

Since the heating rate scales as $E_i^{-1/2}$, where E_i is the energy of incident positrons, the heating from moderated positrons incident on the plasma is significantly higher than that from the unmoderated ones. Taking into account the moderator efficiency, the overall heating from these positrons is comparable to that of the unmoderated ones.

It is necessary to compare this heating rate to $\dot{E}_L$, the rate at which energy is removed from the plasma through laser cooling. We assume a 313 nm laser beam directed perpendicularly to the magnetic field with a 25 μm waist perpendicular to the magnetic axis and 250 μm along the axis, centered on the ion plasma. The laser intensity is adjusted to give a resonant scatter rate of 10 MHz for an ion at the center of the beam. We assume a $^{9}Be^{+}$ cloud of 1 cm in length and 1 mm in diameter rotating at $\omega_r=2\pi(5\ \text{MHz})$. Laser cooling is most efficient using a laser beam propagating along the trap z axis because the Doppler shift associated with the plasma rotation is absent. Experimentally, this would be difficult to realize in the apparatus described here because the positron source and moderator also lie on the z axis. We estimate the laser-cooling rate using Eq. (17) of Ref. [28]. We find that for a laser detuning of 20 MHz and a $^{9}Be^{+}$ plasma temperature of 1 K, $\dot{E}_L\simeq -1000$ eV/s. Since $|\dot{E}_L|\gg|\dot{E}_H|$, the plasma heating from positron impact should not significantly affect the plasma equilibrium.

3. Positron loss

We can estimate the rate at which trapped positrons are lost due to background collisions by scaling the results of Murphy and Surko [29]. In their experiment, positrons were trapped and cooled through collisions with a room-temperature background gas of nitrogen [29]. The trap lifetime was limited to 40 s because of annihilation and positronium formation on the 1.3×10^{-4} Pa (10^{-6} torr) N_2 background. Background gas pressures in room-temperature Penning traps approach 1.3×10^{-8} Pa (10^{-10} torr). If we assume that the cross sections for annihilation on other background gases are similar to that of N_2 [57], our trap lifetime should approach 5 days, long enough to accumulate a significant number of positrons.

We have also estimated the number of positrons ejected from the trap due to large-angle scattering by positrons from the positron source and the moderator. The Rutherford-scattering cross section for these collisions is quite small and the trap loss rate is lower than that of background collisions.

[1] P.J. Schultz and K.G. Lynn, Rev. Mod. Phys. **60**, 701 (1988), and references therein.
[2] T.J. Murphy and C.M. Surko, Phys. Rev. Lett. **67**, 2954 (1991).
[3] L.H. Haarsma, K. Abdullah, and G. Gabrielse, Phys. Rev. Lett. **75**, 806 (1995).
[4] R.G. Greaves and C.M. Surko, Phys. Plasmas **4**, 1528 (1997).
[5] A.P. Mills, Appl. Phys. Lett. **35**, 427 (1979); **37**, 667 (1980).
[6] A.P. Mills, Hyperfine Interact. **44**, 107 (1988).
[7] D.A. Fischer, K.G. Lynn, and D.W. Gidley, Phys. Rev. B **33**, 4479 (1986).
[8] N. Zafar, J. Chevallier, F.M. Jacobsen, M. Charlton, and G. Laricchia, Appl. Phys. A: Solids Surf. **47**, 409 (1988); D.M. Chen, K.G. Lynn, R. Pareja, and Bent Nielsen, Phys. Rev. B **31**, 4123 (1985).
[9] C.M. Surko, M. Leventhal, A. Passner, and F.J. Wysocki, in *Non-neutral Plasma Physics*, edited by C.W. Roberson and C.F. Driscoll (AIP, New York, 1988), p. 75; C.M. Surko, M. Leventhal, and A. Passner, Phys. Rev. Lett. **62**, 901 (1989); T.E. Cowan, J. Hartley, R.H. Howell, J.L. McDonald, R.R. Ronatgi, and J. Fajans, Mater. Sci. Forum **105-110**, 529 (1992).
[10] L. Haarsma, K. Abdullah, and G. Gabriesle, Hyperfine Interact. **76**, 143 (1993); G. Gabrielse, W. Jhe, D. Phillips, R. Kaiser, H. Kalinowsky, and J. Gröbner, Mater. Sci. Forum **105-110**, 75 (1992).
[11] J.M. Wadehra, T.S. Stein, and W.E. Kauppila, Phys. Rev. A **29**, 2912 (1984).
[12] R.S. Conti, B. Ghaffari, and T.D. Steiger, Nucl. Instrum. Methods Phys. Res. A **299**, 420 (1990).
[13] C.F. Driscoll, K.S. Fine, and J.H. Malmberg, Phys. Fluids **29**, 2015 (1986).
[14] J.J. Bollinger, D.J. Heinzen, F.L. Moore, Wayne M. Itano, D.J. Wineland, and D.H.E. Dubin, Phys. Rev. A **48**, 525 (1993).
[15] J.J. Bollinger, L.R. Brewer, J.C. Bergquist, Wayne M. Itano, D.J. Larson, S.L. Gilbert, and D.J. Wineland, in *Intense Positron Beams*, edited by E.H. Ottewitte and W. Kells (World Scientific, Singapore, 1988), p. 63.
[16] D.J. Wineland, C.S. Weimer, and J.J. Bollinger, Hyperfine Interact. **76**, 115 (1993).
[17] H. Boehmer, in *Slow Positron Beam Techniques for Solids and Surfaces*, edited by E. Ottewitte and A. Weiss, AIP Conf. Proc. 303 (AIP, New York, 1994), p. 422.
[18] S.J. Gilbert, C. Kurtz, R.G. Greaves, and C.M. Surko, Appl. Phys. Lett. **70**, 1944 (1997).
[19] J.H. Malmberg and T.M. O'Neil, Phys. Rev. Lett. **39**, 1333 (1977).
[20] G. Gabrielse, S.L. Rolston, L. Haarsma, and W. Kells, Phys. Lett. A **129**, 38 (1988).
[21] M.E. Glinsky and T.M. O'Neil, Phys. Fluids B **3**, 1279 (1991).
[22] G. Gabrielse, W. Jhe, D. Phillips, W. Quint, C. Tseng, L. Haarsma, K. Abdullah, J. Gröbner, and H. Kalinowsky, Hyperfine Interact. **76**, 81 (1993).
[23] P.B. Schwinberg, R.S. Van Dyck, and H.G. Dehmelt, Phys. Lett. **81A**, 119 (1981).
[24] D.S. Hall, Ph.D. thesis, Harvard University, Cambridge, MA, 1997.
[25] G. Gabrielse, J. Estrada. S. Peil, T. Roach. J.N. Tan, and P. Yesley, in *Non-neutral Plasma Physics III*, edited by J.J. Bollinger, R.L. Spencer, and R.C. Davidson (AIP, New York, 1999), p. 29.
[26] B. Ghaffari and R.S. Conti, Phys. Rev. Lett. **75**, 3118 (1995).
[27] A.P. Mills, Jr., in *Positron Scattering in Gases*, edited by J.W. Humberston and M.R.C. McDowell (Plenum Press, New York, 1984), p. 121.
[28] H. Boehmer, M. Adams, and N. Rynn, Phys. Plasmas **2**, 4369 (1995).
[29] T.J. Murphy and C.M. Surko, Phys. Rev. A **46**, 5696 (1992).
[30] C.M. Surko, S.J. Gilbert, and R.G. Greaves, in *Non-neutral Plasma Physics III*, edited by J.J. Bollinger, R.L. Spencer, and R.C. Davidson (AIP, New York, 1999), p. 3.
[31] L.R. Brewer, J.D. Prestage, J.J. Bollinger, Wayne M. Itano, D.J. Larson, and D.J. Wineland, Phys. Rev. A **38**, 859 (1988).
[32] For reviews, see D.J. Wineland, Wayne M. Itano, J.C. Bergquist, J.J. Bollinger, and J.D. Prestage, in *Atomic Physics 9*, edited by R.S. Van Dyck, Jr. and E.N. Fortson (World Scientific, Singapore, 1985), p. 3; W.D. Phillips, J.V. Prodan, and H. Metcalf, *ibid.*, p. 338, and references therein.
[33] D.J. Larson, J.C. Bergquist, J.J. Bollinger, Wayne M. Itano, and D.J. Wineland, Phys. Rev. Lett. **57**, 70 (1986).
[34] J.D. Jackson, *Classical Electrodynamics* (John Wiley and Sons, New York, 1975).
[35] W.R. Leo, *Techniques for Nuclear and Particle Physics Experiments* (Springer-Verlag, New York, 1987), p. 44.
[36] K. Nanbu, Phys. Rev. E **55**, 4642 (1997).
[37] D.J. Heinzen, J.J. Bollinger, F.L. Moore, Wayne M. Itano, and D.J. Wineland, Phys. Rev. Lett. **66**, 2080 (1991).
[38] X.-P. Huang, J.J. Bollinger, T.B. Mitchell, and W.M. Itano, Phys. Rev. Lett. **80**, 73 (1998).
[39] X.-P. Huang, J.J. Bollinger, T.B. Mitchel, W.M. Itano, and D.H.E. Dubin, Phys. Plasmas **5**, 1656 (1998).
[40] We thank T. M. O'Neil, U. C. San Diego for pointing out this mechanism for positron loss.
[41] D.J. Wineland, R.E. Drullinger, and F.L. Walls, Phys. Rev. Lett. **40**, 1639 (1978); W.M. Itano and D.J. Wineland, Phys. Rev. A **25**, 35 (1982).
[42] W.M. Itano, L.R. Brewer, D.J. Larson, and D.J. Wineland, Phys. Rev. A **38**, 5698 (1988).
[43] D.T. Britton, P.A. Huttunen, J. Måkinen, E. Soininen, and A. Vehanen, Phys. Rev. Lett. **62**, 2413 (1989).
[44] Alternatively, the positron source and moderator could be kept on axis behind one endcap by using a thin crystal film transmission moderator. However, the transmitted positron energy spread is heavily dependent on the foil quality and thickness.
[45] C.A. Murray and A.P. Mills, Jr., Solid State Commun. **34**, 789 (1980); R.J. Wilson, Phys. Rev. B **27**, 6974 (1983).
[46] T.M. O'Neil, Phys. Fluids **24**, 1447 (1981).
[47] M.E. Glinsky, T.M. O'Neil, M.B. Rosenbluth, K. Tsuruta, and S. Ichimaru, Phys. Fluids B **4**, 1156 (1992).
[48] S.L. Gilbert, J.J. Bollinger, and D.J. Wineland, Phys. Rev. Lett. **60**, 2022 (1988).
[49] F. Reif, *Fundamentals of Statistical and Thermal Physics* (McGraw-Hill, New York, 1965), p. 273.
[50] X. Krall and X. Trivelpiece, *Principles of Plasma Physics* (McGraw-Hill, New York, 1992), p. 1156.
[51] In Ref. [16], a distribution $P(\theta)d\theta \propto \exp(\theta^2/\langle\theta^2\rangle)d\theta$ was assumed whereas the distribution $P(\theta)d\theta \propto \exp(\theta^2/\langle\theta^2\rangle)\sin\theta d\theta$ should have been used. Assuming small angles ($\sin\theta \simeq \theta$), Eq.

(9) of Ref. [16] should read $\eta_c = \exp(-\theta^2/\Delta\theta_s^2)$, where $\Delta\theta_s^2 = \langle\theta^2\rangle$. This does not significantly affect the results stated in Table 1 of Ref. [16], except for the last value of η_c, which is overestimated.

[52] C.F. Driscoll and J.H. Malmberg, Phys. Rev. Lett. **50**, 167 (1983); F. Anderegg, E. Sarid, and C.F. Driscoll, Bull. Am. Phys. Soc. **38**, 1971 (1993).

[53] B.M. Jelenkovic, T.B. Mitchell, J.J. Bollinger, X.-P. Huang, W.M. Itano, A.S. Barton, and D.J. Wineland, Bull. Am. Phys. Soc. **43**, No. 8, 1653 (1998).

[54] H. Tawara and T. Kato, At. Data Nucl. Data Tables **35**, 167 (1987).

[55] E. Morenzoni, in *Collisions of Antiparticles with Atoms*, edited by D. Berenyi and G. Hock (Springer-Verlag, Berlin, 1991), p. 173.

[56] H.S.W. Massey, E.H.S. Burhop, and H. B. Gilbody, *Electronic and Ionic Impact Phenomena* (Oxford University Press, London, 1974), Vol. V, p. 3125.

[57] P.A. Fraser, in *Advances in Atomic and Molecular Physics 4* (Academic Press, New York, 1968), p. 63.